

# Photoemission Spectroscopy from Inhomogeneous Models of Cuprates

J. Eroles<sup>1,2</sup>, G. Ortiz<sup>1</sup>, A. V. Balatsky<sup>1</sup> and A. R. Bishop<sup>1</sup>

<sup>1</sup>*Theoretical Division, Los Alamos National Laboratory, Los Alamos, NM 87545, USA.*

<sup>2</sup>*Centro Atómico Bariloche and Instituto Balseiro, S. C. de Bariloche, Argentina.*

(Received November 3, 2018)

We investigate the electronic dynamics in the underdoped cuprates focusing on the effects of one-dimensional charge stripes. We address recent experimental Angular-Resolved Photoemission Spectra results on  $(\text{La}_{1.28}\text{Nd}_{0.6}\text{Sr}_{0.12})\text{CuO}_4$ . We find that various inhomogeneous models can account for the distribution of quasiparticle weights close to momentum  $\mathbf{k} = (\pi, 0)$  and symmetry related points. The observed flat dispersion region around the same  $\mathbf{k}$  point can only be addressed by certain classes of those inhomogeneous models which locally break spin symmetry. Homogeneous models including hopping elements up to second neighbors cannot reproduce the experimental quasiparticle weight, since most of it is centered around  $\mathbf{k} = (\frac{\pi}{2}, \frac{\pi}{2})$ .

Recent interest in the inhomogeneous states of high- $T_c$  superconductors has gained further impetus from new experiments that support charged stripe formation. One set of data is available on the Nd-doped LSCO [1] and, more recently, a second set concerns oxygen doped LSCO [2]. Angular-Resolved Photoemission Spectra (ARPES) obtained on the commensurate-doped Nd LSCO [3] revealed that the electronic spectra, believed to contain static stripes, are consistent with the electronic states having quasi-one-dimensional (1D) character.

The question that naturally arises from these measurements is: what are the most appropriate models that can capture both the formation of the stripes and adequately describe the spectroscopic features of the electronic states in these compounds? The issue of the physics that drives stripe formation is a matter of extensive current debate [4], with a number of models that can describe the static and dynamical stripe formation.

Faced with the new experimental data, we choose here a different approach. We assume from the beginning that the Hamiltonian for our model is inhomogeneous to mimic the effects of stripes. As a consequence the electronic states will be quite different from the conventional homogeneous models, such as a  $tt'$ - $J$  model. We find that suitable explicitly inhomogeneous models allow a good fit to the ARPES data, and capture the main qualitative features that are consistent with a quasi-1D nature of electronic states on the stripes.

The inhomogeneous models we will consider have already been introduced in Ref. [5], where the basic microscopic scenario starts from a homogeneous  $t$ - $J$  Hamiltonian as a reference background model:

$$H_{t-J} = -t \sum_{\langle \mathbf{r}, \bar{\mathbf{r}} \rangle, \sigma} c_{\mathbf{r}\sigma}^\dagger c_{\bar{\mathbf{r}}\sigma} + J \sum_{\langle \mathbf{r}, \bar{\mathbf{r}} \rangle} (\mathbf{S}_{\mathbf{r}} \cdot \mathbf{S}_{\bar{\mathbf{r}}} - \frac{1}{4} \bar{n}_{\mathbf{r}} \bar{n}_{\bar{\mathbf{r}}}). \quad (1)$$

We have also considered the  $tt'$ - $J$  model which includes hopping elements up to second neighbors. To mimic the stripe segments, we add specifically inhomogeneous *magnetic* interactions. These inhomogeneous terms locally

break translational invariance and spin-rotational  $SU(2)$  symmetry:

$$H_{\text{inh}} = \sum_{\langle \alpha, \beta \rangle} \delta J_z S_\alpha^z S_\beta^z + \frac{\delta J_\perp}{2} (S_\alpha^+ S_\beta^- + S_\alpha^- S_\beta^+). \quad (2)$$

Here  $\delta J_\perp \neq \delta J_z$ , represents the magnetic perturbation of a static, local, *Ising* anisotropy, locally lowering spin symmetry (termed a  $t$ - $JJ_z$  model [5]). Only a few links (where the stripes are located) have this lowered spin symmetry. The Ising anisotropy is also sufficient to produce a spin gap [5] and pair binding of holes in this class of models is substantial [5]. An alternative scenario for stripe segments can be realized through inhomogeneous terms of the form

$$\tilde{H}_{\text{inh}} = - \sum_i \epsilon_i (1 - \bar{n}_i), \quad (3)$$

where  $\epsilon_i > 0$  represents an on-site orbital energy which is non-vanishing only at the stripe sites  $i$  ( $tt'$ - $J\epsilon_i$  model). ARPES signal of the noninteracting electron model with external potential, consistent with the stripe pattern, has been previously addressed in Ref. [6]. The spin rotation symmetry is not broken in this case. This kind of model resembles, although is different, to that studied in Ref. [7], where it was shown to reproduce experimental neutron magnetic scattering, optical conductivity and the ARPES measured broad spectrum near  $\mathbf{k} = (\frac{\pi}{2}, \frac{\pi}{2})$  along the direction  $(0, 0) - (\pi, \pi)$  [7].

In the rest of this paper the energy scale will be determined by  $t$ . As we will vary the magnitude of the spin anisotropy [5], we choose to fix  $J/t = 1$ . This is a little higher than the commonly assumed value for homogeneous cuprate systems of  $J/t = 0.4$ , but close enough to be physical. It is not our purpose here to define an energy scale which can be related to the experiments, but rather to demonstrate that the main aspects of the experiments can be address by particular kinds of models. Systematic tuning of the parameters will be published elsewhere.

Recent ARPES experiments in  $\text{La}_{1.28}\text{Nd}_{0.6}\text{Sr}_{0.12}\text{CuO}_4$  seem to indicate a 1D electronic structure [3]. At low transferred energies and integrating the spectral weight within a 100 meV window ( $\Delta\omega = 100$  meV), the quasiparticle weight looks like that depicted in Figs. 1 and 2. Basically, there is almost no weight at  $\mathbf{k} = (\frac{\pi}{2}, \frac{\pi}{2})$ , and most of the weight is concentrated near the point  $\mathbf{k} = (\pi, 0)$ . Moreover, one can see from the quasiparticle band structure that there is almost no dispersion in  $k_y$ . Besides, there is a flat band for large  $k_x$  that can be related to a velocity scale [8]. By integrating the same data over a window of 500 meV ( $\Delta\omega = 500$  meV), the experimental spectrum is like that in Fig. 4. There is no peak at  $\mathbf{k} = (\frac{\pi}{2}, \frac{\pi}{2})$  and most of the spectral weight is transferred from  $\mathbf{k} = (\pi, 0)$  to  $\mathbf{k} = (\frac{\pi}{2}, 0)$  and symmetrically equivalent points. Both cases ( $\Delta\omega = 100$  meV or 500 meV) are characteristic of a 1D behavior of the electronic degrees of freedom [3]. These experiments were all performed at a commensurate hole filling corresponding to  $x = 1/8$ .

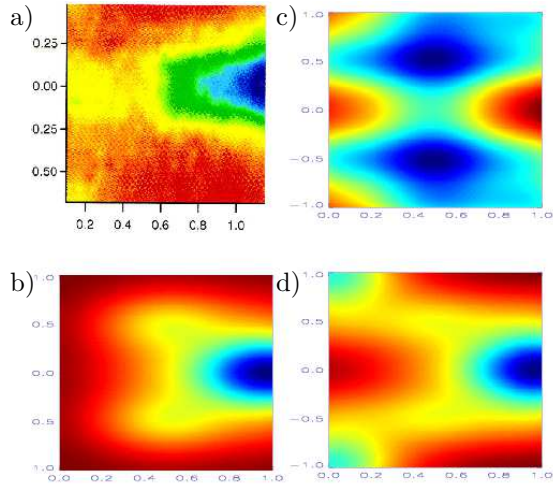


FIG. 1. (a) Experimental ARPES from [3]. (b), (c) and (d) correspond to the unsymmetrized calculated spectrum for  $t$ - $JJ_z$ ,  $tt'$ - $J$  and  $tt'$ - $J\epsilon_i$  models, respectively. Note that no integral of spectral weight has been taken yet.

Our goal here is to study different homogeneous and inhomogeneous models and compare to the experimental dynamic properties measured in Ref. [3]. We used the Lanczos numerical exact diagonalization method on a  $4 \times 4$  cluster (see inset Fig. 6). When stripes are present, the Hamiltonian along one leg is modified by adding the inhomogeneous terms (like in Eqs. 2 or 3).

The spectral function we need to compute is given by

$$\mathcal{A}(\mathbf{k}, \omega) = \sum_n |\langle \Psi_n^{\nu+1} | c_{\mathbf{k}\sigma}^\dagger | \Psi_0^\nu \rangle|^2 \delta(\omega - (E_n^{\nu+1} - E_0^\nu)) , \quad (4)$$

where  $|\Psi_n^\nu\rangle$  corresponds to an eigenstate of the Hamiltonian in the subspace of  $\nu$  holes with energy  $E_n^\nu$ . The first poles of the corresponding Green's function define the quasiparticle weight through the intensity, and the energy associated to that quasiparticle through the position of the poles. As the experiments in Ref. [3] are at  $x = 1/8$ , we carried out the simulations with one hole added to a background where there was already one hole present ( $\nu = 1$ ). For our 16 sites cluster, the final concentration then corresponds to  $x = 1/8$ .

Since our system is finite, we can only consider a finite set of  $\mathbf{k}$  values in the Brillouin zone. These are:  $\mathbf{k} = (k_x, k_y)$  with  $k_{x,y} = 0, \pm\frac{\pi}{2}, \pm\pi$ . To compare with experimental results we associate a Gaussian with a small width ( $\sigma \simeq 0.1$ ) centered at each computed  $\mathbf{k}$  point and with a height corresponding to the spectral weight for that  $\mathbf{k}$  point. Finally, we sum all these Gaussians centered at the  $\mathbf{k}$  values of our finite lattice. The resulting field is color coded with blue corresponding to maxima and red to minima. For each graph the maximum is scaled to 1.

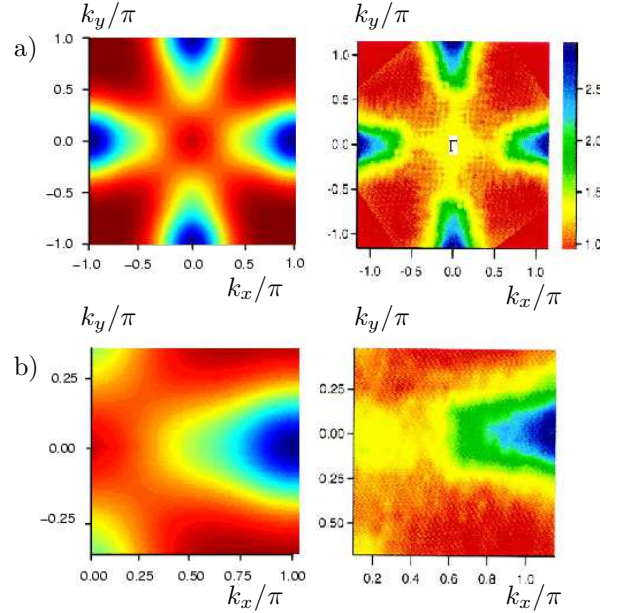


FIG. 2. Comparison between the inhomogeneous  $t$ - $JJ_z$  model ( $t/J = 1$  and  $\delta J_\perp = -0.9$ ) integrated up to  $\Delta\omega = 0.13t$  (left) and ARPES experimental results (right) from [3] integrated over  $\Delta\omega = 100$  meV. (a) Four quadrants view (b). Zoom of the zone around  $(\pi, 0)$ .

In Fig. 1 we show (a) the experimental spectrum from Ref. [3] and the corresponding unsymmetrized model predictions for (b)  $t$ - $JJ_z$ , (c)  $tt'$ - $J$  and (d)  $tt'$ - $J\epsilon_i$  models. For the calculations we have taken the first quasiparticle pole for each  $\mathbf{k}$  point. (Note that for some  $\mathbf{k}$  points the weight is very small). Clearly predictions from the

inhomogeneous models ((b) and (c)) are qualitatively different from the homogeneous  $tt'-J$  model. In both inhomogeneous cases the weight is concentrated around  $\mathbf{k} = (\pi, 0)$  as in the experimental ARPES. But if stripes are present, the experiment averages domains with different stripe orientations. Therefore, in order to compare with the experiments, we symmetrize the numerical results by taking the average with the rotated spectrum and integrating the results in a frequency window  $\Delta\omega$  for each  $\mathbf{k}$  point, as was done in Ref. [3].

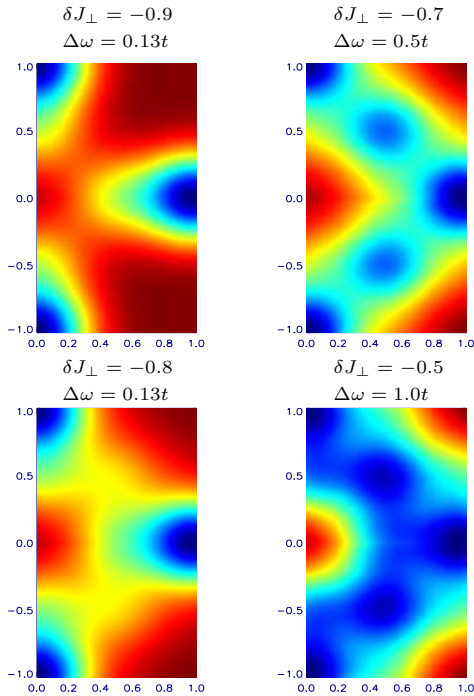


FIG. 3. Spectra for different parameters and integration windows for the  $t-JJ_z$  model. As the strength of the stripe is decreased ( $\delta J_\perp \rightarrow 0$ , making the model more homogeneous) noticeable weight is transferred to  $\mathbf{k} = (\frac{\pi}{2}, \frac{\pi}{2})$  and to the boundary of the “ghost” Anti-Ferromagnetic Brillouin zone.

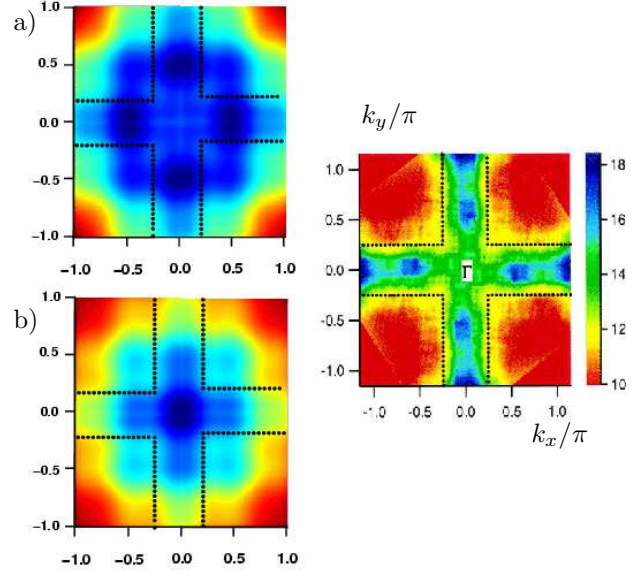


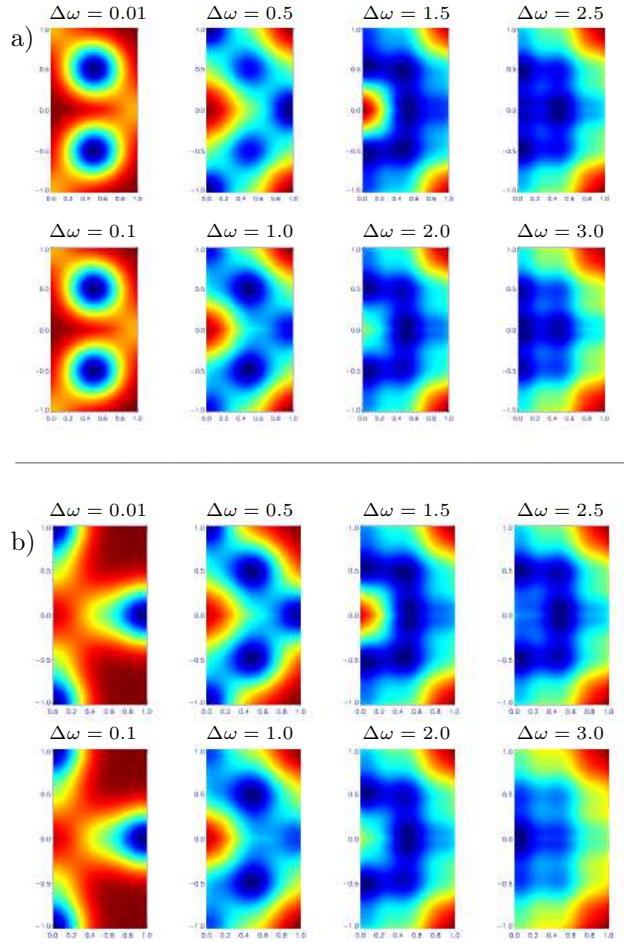
FIG. 4. Comparison between the inhomogeneous  $t-JJ_z$  model ( $t/J = 1$  and  $\delta J_\perp = -0.9$ ) (left) and ARPES experimental results (right) [3] integrated in a 500 meV range. Four quadrants view. (a)  $\Delta\omega = 2.5t$ ; (b)  $\Delta\omega = 3.5t$ .

In Fig. 2 we compare the calculated spectra in the inhomogeneous  $t-JJ_z$  model (Eq. 2), where the stripes are represented as local *Ising* anisotropy, symmetrized and integrated over a range up to  $\Delta\omega = 100$  meV. The Hamiltonian corresponds to Eqs. 1 and 2 with  $\delta J_\perp = -0.9$ . Figure 2 corresponds to (a) the full 4 quadrants view, and (b) to a partial view around  $\mathbf{k} = (\pi, 0)$ . The agreement is very good. In the experiment significant spectral weight was found around  $\mathbf{k} = (0, 0)$ . Our data, on the other hand, do not show any significant weight at  $\mathbf{k} = (0, 0)$ . It is well known that the reduction to one band effective models is not very good at this  $\mathbf{k}$  point [9]. Thus the lack of weight at  $\mathbf{k} = (0, 0)$  is a consequence of the reduction to the  $t-J$  model and not important for our present considerations.

In Fig. 3 we display the quasiparticle weights for various values of the stripe anisotropy. Note the transfer of weight from  $\mathbf{k} = (\pi, 0)$  to  $\mathbf{k} = (\frac{\pi}{2}, \frac{\pi}{2})$  as the system becomes more homogeneous.

Quasiparticle features involving many sites (and therefore with higher energies) will not be properly captured in our small cluster. Nevertheless, it still seems able to describe the main trends as the window of integration in the experiment is raised to  $\Delta\omega = 500$  meV. As seen in Fig. 4(a) the weight concentrates around  $\mathbf{k} = (\frac{\pi}{2}, 0)$  and equivalent points, even though the weight at  $\mathbf{k} = (\frac{\pi}{2}, \frac{\pi}{2})$  is still significant. As the window of integration is raised to  $\Delta\omega = 3.5t$ , most of the weight is concentrated between  $\mathbf{k} = (0, 0)$  and  $\mathbf{k} = (\frac{\pi}{2}, 0)$ . Probably because of the size of our cluster, none of the models studied can exactly

reproduce the features of this high energy profile; indeed as expected, they are all very similar in this range.



In Fig. 5 we compare the distribution of quasiparticle weights for homogeneous  $tt'-J$  and inhomogeneous  $t-JJ_z$  models after symmetrization and for different integration windows  $\Delta\omega$ . We study the  $tt'-J$  model since it is well known that, in our cluster, the bare  $t-J$  has a hidden symmetry for 1 hole that makes  $\mathbf{k} = (\pi, 0)$  and  $\mathbf{k} = (\frac{\pi}{2}, \frac{\pi}{2})$  degenerate. In particular for a chain, the dispersion relation for a  $t'$  term is  $\epsilon_k = -2t' \cos(2k)$ , and therefore it lowers the quasiparticle energy at both  $k = 0$  and, more importantly, at  $k = \pi$ . If for some reason the system has a 1D (or quasi 1D) behavior, this  $t'$  term will transfer quasiparticle weight from  $k = \frac{\pi}{2}$  to  $k = \pi$ , as observed in the experiments. From Fig. 5 it can be seen that in the homogeneous model the experimental weights cannot be reproduced by  $t'/t = -0.3$  (the commonly assumed value for  $t'$  [10]) for any  $\Delta\omega$ . It is also interesting to note that in the inhomogeneous  $tt'-J\epsilon_i$  model, after symmetrization, the prominent peak at  $\mathbf{k} = (\pi, 0)$  and equivalent points (as in Fig. 5(b) for  $\Delta\omega = 0.01t$  and  $\Delta\omega = 0.1t$ ) is comparable to  $\mathbf{k} = (\frac{\pi}{2}, \frac{\pi}{2})$  for most of the  $\Delta\omega$  window sizes. Therefore the agreement with experiments is poor. For large  $\Delta\omega$  all the models are very much alike. This is to be expected since if the stripe perturbation is small enough, only the low energy states change significantly, and therefore all inhomogeneous and homogeneous models give the same qualitatively spectra for sufficiently large  $\Delta\omega$ .

FIG. 5. Comparison of the spectral density between (a) homogeneous  $tt'-J$  ( $t' = -0.3t$ ) and (b) inhomogeneous  $t-JJ_z$  ( $t/J = 1$  and  $\delta J_\perp = -0.9$ ) models. Blue corresponds to maximum intensity and red to minimum. Each plot corresponds to the indicated range of integration  $\Delta\omega$  (in units of  $t$ ).

As mentioned earlier, another distinctive feature in the ARPES experiments is the flat dispersion around  $\mathbf{k} = (\pi, 0)$ . This flat region may be associated with a velocity which in turn defines the linear relation between the separation between stripes and the superconducting transition temperature [8]. Therefore it is important to see if the flat region is present in our models. In Fig. 6 we show the position of the first pole for each model, for the  $\mathbf{k}$  points along the  $(0, 0) - (\frac{\pi}{2}, 0) - (\pi, 0)$  line. The  $t-JJ_z$  and  $tt'-J$  models are flat enough to be consistent with the experiment, but as we have seen above, the latter cannot account for the weight distribution (see Fig. 5). On the other hand the model labeled as  $tt'-J\epsilon_i$  does not show the flat dispersion. This is a further indication that even though inhomogeneities are necessary to account for the ARPES experiments, not all kinds of inhomogeneities are appropriate.



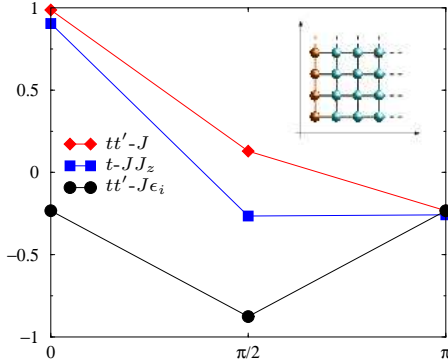


FIG. 6. Dispersion relation for the different models along the  $(0,0) - (\frac{\pi}{2},0) - (\pi,0)$  line. The experimentally observed flat band close to  $\mathbf{k} = (\pi,0)$  [3] is well reproduced by the  $t$ - $JJ_z$  and  $tt'$ - $J$  models.

In conclusion, we have calculated the ARPES response in several inhomogeneous and homogeneous models. We used exact diagonalization in a cluster with  $C_{4v}$  symmetry and hole doping appropriate to  $x = \frac{1}{8}$ . We found that the experimentally measured quasiparticle peak near  $\mathbf{k} = (\pi,0)$  and symmetry equivalent points is well reproduced only by the inhomogeneous models. We also find that for all models, some weight peaked at  $\mathbf{k} = (\frac{\pi}{2}, \frac{\pi}{2})$ . It is of comparable intensity (although usually smaller) to the peak at  $\mathbf{k} = (\pi,0)$ , and is present for some integration windows. Of those models we studied, only those that locally break  $SU(2)$  symmetry can also explain the experimentally observed flat dispersion around this same  $\mathbf{k}$  point. We note that this same model has a spin-gap,

substantial binding of holes and exhibits an incommensuration in the spin structure factor [5]. It thus appears to capture many important experimental features in the electronic, magnetic and potentially superconducting channels.

Preliminary results of this work were presented on the M2S-HTSC-IV conference in Houston [11]. Subsequent to completion of this work we learn about a recent preprint by D. Orgad *et al.* (cond-mat/0005457) and by M.G. Zacher *et al.* (cond-mat/0005473), where the relationship between stripe patterns and ARPES data is discussed. We thank A.A. Aligia, S. Kivelson, Z-X. Shen and X.J. Zhou for useful discussions. Work at Los Alamos is sponsored by the US DOE under contract W-7405-ENG-36.

- 
- [1] Tranquada *et al.*, Phys. Rev. B **59**, 14712 (1999); Tranquada *et al.*, Phys. Rev. Lett **78**, 338 (1997).
  - [2] S. Wakimoto *et al.*, cond-mat/9908115.
  - [3] X.J. Zhou *et al.*, Science 286, (1999) 268 and private communication.
  - [4] S.R. White and D.J. Scalapino, Phys. Rev. Lett. **80** 1272 (1998); G. Seibold, C. Castellani, C. Di Castro and M. Grilli, Phys. Rev. B **58**, 13506 (1998); A. Sadori and M. Grilli, cond-mat/9907447; C.S. Hellberg and E. Manousakis, Phys. Rev. Lett. **83**, 132 (1999).
  - [5] J. Eroles, G. Ortiz, A.V. Balatsky, and A.R. Bishop, Europhys. Lett. **50**, 540 (2000).
  - [6] M.I. Salkola *et al.*, Phys. Rev. Lett. **77**, 155 (1996).
  - [7] T. Tohyama, S. Nagai, Y. Shibita and S. Maekawa, Phys. Rev. Lett. **82**, 4910 (1999).
  - [8] A.V. Balatsky and P. Bourges, Phys. Rev. Lett. **82**, 5337 (1999); A.V. Balatsky and Z.-X. Shen, Science **284**, 1137 (1999).
  - [9] J. Eroles, C.D. Batista and A.A. Aligia, Phys. Rev. B **59**, 14092 (1999).
  - [10] C.D. Batista and A.A. Aligia, Phys. Rev. B **48**, 4212 (1993).
  - [11] J. Eroles, G. Ortiz, A.V. Balatsky, and A.R. Bishop, Physica C (in press); cond-mat/0003322.